Image Data Analysis for Quantifying Scar Tissue Transmurality in Cardiac Resynchronisation Therapy

Rashed Karim[1], Maria Panayiotou[1], Onik Chowdhury[1], R. James Housden[1], Sana Hummady[2], Daniel Toth[4], Tanja Kurzendorfer[2], Peter Mountney[3] and Kawal Rhode[1]

***Abstract*— The use of implantable cardiac devices has increased in the last 30 years. Cardiac resynchronisation therapy (CRT) is a procedure which involves implanting a coin sized pacemaker for reversing heart failure. The pacemaker electrode leads are implanted into cardiac myocardial tissue. The optimal site for implantation is highly patient-specific. Most implanters use empirical placement of the lead. One region identified to have a poor response rate are myocardial tissue with transmural scar. Studies that precisely measure transmurality of scar tissue in the left ventricle (LV) are few. Most studies lack proper validation of their transmurality measurement technique. This study presents an image analysis technique for computing scar transmurality from late-gadolinium enhancement MRI. The technique is validated using phantoms under a CRT image guidance system. The study concludes that scar transmurality can be accurately measured in certain situations and validation with phantoms is important.**

I. INTRODUCTION

Patients with symptomatic heart failure are commonly treated with procedures such as Cardiac resynchronization therapy (CRT) by implanting a pacemaker for the heart. In this procedure, the electrode leads of the pacemaker are implanted in myocardial tissue to artificially pace the heart. Pacing sites are now being assessed for tissue scarring in order to determine sites that will be responsive to lead placement. The extent of tissue damage or scarring at potential pacing sites is a novel way of performing this assessment [1]. The ultimate goal is to provide a CRT that is patient-specific and hence more effective.

The extent of scarring in cardiac myocardium is also often termed as *transmurality* of scar. A fully transmural scar runs along the myocardium. It is challenging to measure transmurality as it must be measured in all three spatial directions from a pixelated three dimensional (3D) reconstructed image of scar. magnetic resonance imaging (MRI) remains the gold-standard for cardiac tissue characterisation. An MRI imaging technique known as late Gadolinium enhancement (LGE) provides 3D visualisation of cardiac tissue with a relative high intensity within scarred areas. Scar assessment with LGE imaging prior to CRT lead placement has shown to improve patient outcomes [1] in these procedures and transmurality is increasingly being seen as an important scar metric.

[1]R. Karim, M. Panayiotou, O. Chowdhury, R.J. Housden and K. Rhode are with School of Biomedical Engineering & Imaging Sciences, King's College London, London, United Kingdom

[2]S. Hummady and T. Kurzendorfer are with Siemens Healthineers, Forchheim, Germany

[3]P. Mountney is with Siemens Healthineers, Medical Imaging Technologies, Princeton, NJ, USA

[4]D. Toth is with Siemens Healthineers, Frimley, UK

A. Previous works

There is little literature on the topic of scar transmurality computation and validation is almost always performed using visual assessment. In [2], authors employed a hysteresis thresholding method to assess scar transmurality. Transmurality was scored using a five-point scale (0: no infarction; 1: transmural $< 25\%$; 2: transmural from 26% to 50%; 3: transmural from 51% to 75%; 4: transmural from 76% to 100%) and the study found that transmurality was generally scored lower when compared to visual assessment.

In a separate study [3], transmurality was calculated by dividing the ventricular wall with several equidistant chords ($n = 100$). Signal intensity was analysed at ten equidistant points along each chord and increased signal intensity was expressed as a percentage of left ventricular wall thickness. The average was then taken per segment of the 16-segment LV model. The quantitative values of transmurality was compared to visual assessments by two experienced observers scoring transmurality using the 5-point scale.

The authors in [4] calculated scar transmurality from LGE by integrating along radial spikes of myocardium. These spikes are understood to be lines at regular intervals perpendicular to myocardium. The automated approach was compared to transmurality using visual assessment obtained from consensus delineation of scar ($n = 3$ observers). The algorithm found a lower scar transmurality score, on average, compared to visual assessment.

The authors in [5] compared four different methods of scar transmurality. In their study, transmurality was divided into quartiles (1-24%, 25-49%, 50-74% and 75-100%) and scar above 75% was considered as transmural. Images were assessed by an experienced cardiologist and the study found that these methods tended to under-estimate transmurality. The study concluded that transmurality calculations could vary significantly depending on the chosen method and further studies were necessary to obtain a validated and consensual study method.

B. Motivation

The literature survey indicates the need for a well validated approach for computing transmurality. Furthermore, the development of a state-of-the-art CRT planning and navigation platform within our lab [6] enabled this proposed image

analysis technique for scar transmurality to be validated within an actual CRT image guidance environment.

II. MATERIALS AND METHODS

A. Image Analysis

An important pre-requisite for measuring transmurality is to obtain a visualisation of the myocardium including scar. To visualise myocardium, the LV was imaged along its short-axis (SA) and long-axis (LA) with cine MRI imaging. The contours of myocardium representing its outer and inner layers were extracted using probabilistic analysis of image intensity gray levels [6]. To visualise scar, the LV was imaged with LGE MRI. The cine SA and LA was registered to the LGE MRI using normalised mutual information (NMI) to reveal myocardium in the LGE. This was necessary as it cannot be accurately delineated alone with LGE. Image pixels within scarred areas were obtained by thresholding image intensity to three standard deviations from mean healthy tissue.

The LV was divided into the 3D 16-segment American Heart Association (AHA) model (see Fig 1), which is a standard for CRT procedures to determine segments that can be selected for placing pacemaker leads. Within every segment, transmurality was computed for determining the scar extent. Each segment covered a portion of the LGE image. The segments were further sub-divided into smaller *sectors* such that transmurality could be calculated for each sector and averaged over all sectors to give a more accurate representation of scar extent. Fig. 2 provides an illustration of a sector within a segment.

Sectors were defined at θ intervals within each segment, where $\theta = 10^\circ$ as illustrated in Fig. 2. Within each sector, transmurality could be calculated by computing the ratio between the width of scar and width of myocardium in that sector. The width of scar was defined as the distance between the nearest (S_{min}) and the farthest (S_{max}) scar pixels from LV centre: $S_{max} - S_{min}$. The width of myocardium could be obtained directly from the extracted contours. Transmurality T is given by:

$$T_k = \frac{1}{n} \sum \frac{S_{max} - S_{min}}{M_{max} - M_{min}} \quad (1)$$

where $M_{max} - M_{min}$ is width of myocardium calculated from its contours and averaging the distance ratios over all n sectors to obtain transmurality for the k^{th} segment (Eq. 1). Fig. 2 illustrates how transmurality could be calculated in an individual sector within a single segment of the LV's 16-segment model using Eq. 1.

B. Phantom Validation

It is impossible to validate the extent of scar being measured using image analysis in patients undergoing CRT. The absolute truth on the scar's extent even with post-mortem histology has been known to pose challenging conditions as a result of the tissue fixing process, an essential preservation step that alters structural properties of tissue. However, it may be possible to validate image analysis using phantoms

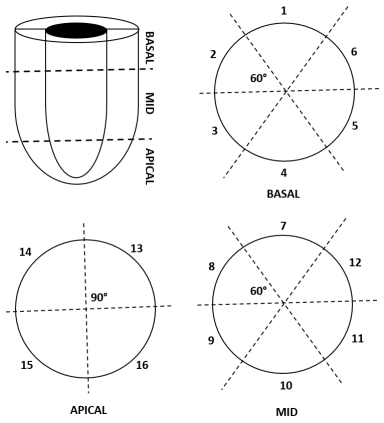

Fig. 1: The sub-division of the left ventricle into 16 segments (outer boundary labels). Segments are subdivided into 60° segments in the basal and mid layers, and 90° segments in the apical or apex layer.

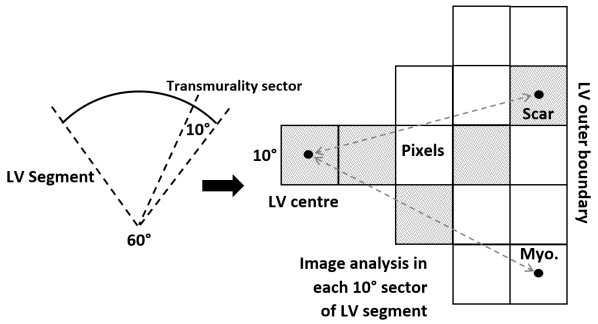

Fig. 2: A schematic diagram for transmurality calculations within each $\theta = 10^\circ$ sector of a single segment of the LV (left). The instance in this example has 100% transmurality, due to scar's extent from centre to outer boundary, with distances indicated between LV centre and outermost scar and myocardium (Myo.) pixels.

and this is a common approach. Heart phantoms can be constructed from realistic 3D models and printed with rapid 3D prototyping using only MRI-safe material. The phantom could be imaged with MRI making it possible to calculate and compare scar transmurality with ground truth.

In this work, an LV phantom was designed with open-source Blender 3D software (Blender Foundation). The dimensions were 55 x 65 mm to allow it to be imaged sufficiently in low-resolution MRI, where a slice thickness of 8 mm allowed between 9-11 slices. The phantoms contained compartments for housing poly-vinyl alcohol (PVA) gel to represent scar. There were three concentric compartments for housing the gel at 33%, 66% and 100% transmurality. The phantom could only be imaged once the PVA gel reached a state to give it a scar-like intensity in MRI imaging. To attain this state, the PVA gel underwent a freeze/thaw cycle at -35C/+20C as described in [7]. It was possible to generate five different configurations of transmurality by using different combinations of compartments in the phantom. These

configurations allowed transmurality to be validated at: 1) 33%, 2) 66%, 3) 66% using mid and outer compartment, 4) 100%, 5) 100% by leaving an empty mid compartment. Fig. 3 gives a display of all the instances.

C. Phantom Imaging

The phantoms were immersed in water to better distinguish and visualise the PVA gel from the phantom's plastic wall. Due to the solid nature of plastic there were no free Hydrogens to produce an MRI signal. The signal void from the plastic walls against the high signal provided by pure water was utilised to visualise the phantom more clearly. The imaging technique used was LGE, the same technique used to image myocardium scar in CRT patients. The LGE imaging resolution was 1.7×1.7 mm in-plane with slice thickness of 8 mm. The phantoms were imaged inside a catheter lab within an actual CRT guidance platform environment equipped with X-Ray and MRI imaging capabilities (Siemens Healthineers, Erlangen, Germany). The platform was used to align the phantom to typical patient orientation, allowing Cine MRI to LGE image registration followed by scar reconstruction within the CRT procedure workflow. A description of such a workflow can be found in [6].

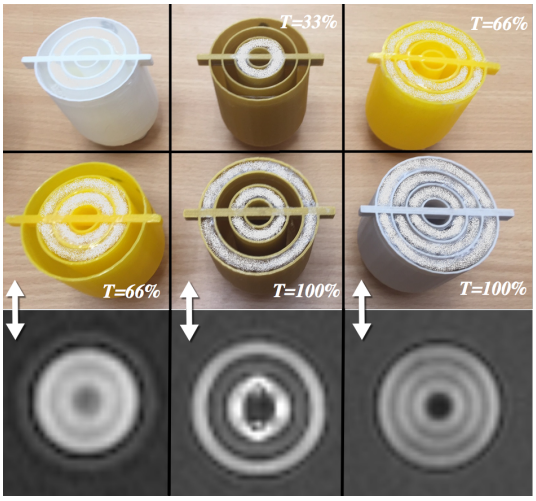

Fig. 3: Phantoms used in validation, with PVA gel filling to simulate five separate configurations of scar transmurality (T) with their corresponding LGE images (short-axis slice) for three phantoms. Top-left: phantom before PVA freeze/thaw cycle

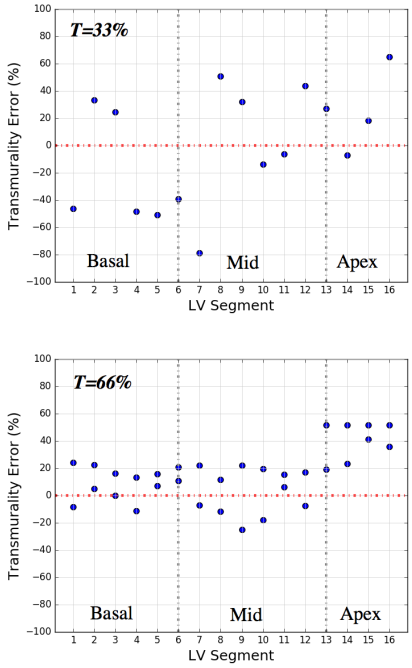

Fig. 4: Error in transmurality measurements using image analysis in phantoms. Each subplot represents a transmurality configuration ($T = 33, 66\%$) used in validation. Note the plot for $T = 100\%$ is omitted as image analysis had a near perfect accuracy

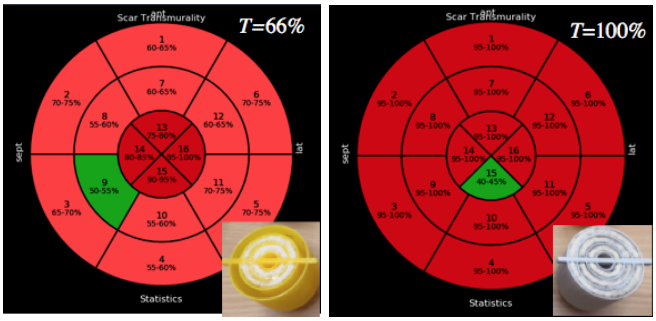

Fig. 5: Bull's eye visualisation of the 16-segment LV model in the validation phantoms (inset) used in this study. The percentage transmurality using image analysis is noted within each segment

III. RESULTS

Transmurality was computed using image analysis within each segment of the LV in the 16-segment AHA model. These values were compared to actual transmurality that was prepared in the phantoms using PVA gels. For performing this comparison, two metrics were used. Firstly, the mean and median transmurality as computed using image analysis within each layer (basal, mid and apex) of LV was determined (see Table I). Secondly, the percentage error between computed and actual transmurality was calculated for each segment. This is shown in each of the sub-plots of Fig. 4, where each sub-plot represents the level of transmurality being assessed ($T = 33\%$ and $T = 66\%$). Each data point in the plot represents the percentage error in transmurality measurement within a single segment.

The errors within each layer was also determined. For basal, mid and apex these were $13\% \pm 16\%$, $16\% \pm 19\%$, and $25\% \pm 23\%$ respectively. It may be worthwhile to note this could only be obtained from a small number data points in the basal ($n = 32$), mid ($n = 32$), and apex ($n = 16$) layers.

TABLE I: Actual transmurality (T) prepared in the phantom and estimated ($\hat{T}$) using image analysis in each layer of the left ventricle

	Actual	$T = 33$	$T = 66$	$T = 100$
Overall	Mean	$\hat{T} = 33$,	$\hat{T} = 76$	$\hat{T} = 98$
	Median	$\hat{T} = 35$	$\hat{T} = 77$	$\hat{T} = 100$
Basal	Mean	$\hat{T} = 27$,	$\hat{T} = 71$,	$\hat{T} = 99$
	Median	$\hat{T} = 18$	$\hat{T} = 72$	$\hat{T} = 100$
Mid	Mean	$\hat{T} = 34$,	$\hat{T} = 68$,	$\hat{T} = 100$
	Median	$\hat{T} = 37$	$\hat{T} = 72$	$\hat{T} = 100$
Apex	Mean	$\hat{T} = 41$,	$\hat{T} = 92$,	$\hat{T} = 92$
	Median	$\hat{T} = 40$	$\hat{T} = 97$	$\hat{T} = 100$

IV. Discussion

A. Contribution

The main contribution of this work is an image analysis approach for measuring the transmurality of scar from MRI imaging. To our knowledge, although there are image analysis approaches for measuring scar transmurality, they were not validated with phantoms. The MRI images of our phantoms created in this study are now open-source and can be obtained from: `https://github.com/drkarim`

B. Accuracy

It was noted that the accuracy decreased in the apex layers of the LV. This is evident in the plots of Fig. 4 and Table I. As LV diminishes in the apex layer, there are fewer slices that are required to image an even smaller area. This increases the margin of error. The accuracy was significantly better in $T = 100$ and the validation with these phantoms showed far greater accuracy than $T = 33$ and $T = 66$. As such, this image analysis technique had excellent accuracy for detecting fully transmural scar and could potentially be useful for binarising transmurality.

C. Transmurality

There is no consensus agreement on how transmurality should be reported. Reporting it as a percentage of myocardium is common, but whether it portrays the correct information of the underlying tissue state is debatable. It is particularly relevant if scar covers inner and outer myocardium (Fig. 3, 2nd column, $T = 100\%$). In this case, although it could be said that $T = 66\%$, but the inner tissue is unresponsive to CRT due to blockage from scar. A categorial measure for transmurality from percentage could be more relevant.

D. Limitations

Partial volume effect was an important limitation of this study. This introduced errors in the scar reconstruction step, which is a pre-requisite step for transmurality. Partial voluming can be a limiting factor in MRI where the resolution is relatively low compared to other modalities such as CT. However, MRI is the gold-standard for cardiac tissue characterisation and thus the preferred modality for scar assessment. In our study, a resolution of $1.7 \times 1.7 \times 8$ mm was used to image a phantom 55 by 65 mm and this resulted in some blurred boundaries.

There are implications of partial voluming in our work of phantom validation. In some segments, the scar could not be accurately delineated and reconstructed due to unclear boundaries and this resulted in few extra pixels of scar or myocardium. These extra pixels in the phantom's image introduced errors in the image analysis validation process. A perfect accurate representative image of the prepared phantoms could not be obtained. Although, increasing the dimensions of the phantom may alleviate the issue, but that could deviate it from actual cardiac size. It is becoming possible to image cardiac scar with a high spatial resolution, and some images of animal models are now open-source [8]. This, however, remains to be interesting future work.

Acknowledgment

Dr. Karim was supported by the National Institute for Health Research Biomedical Research Centre at Guy's and St. Thomas' NHS Foundation Trust and King's College London. The authors are grateful for the support from the Innovate UK grant 32684-234174. Concepts and information presented are based on research and are not commercially available. Due to regulatory reasons, the future availability cannot be guaranteed.

References

[1] J. M. Behar, P. Mountney, D. Toth, S. Reiml, M. Panayiotou, A. Brost, B. Fahn, R. Karim, S. Claridge, T. Jackson, *et al.*, "Real-time x-mri-guided left ventricular lead implantation for targeted delivery of cardiac resynchronization therapy," *JACC: Clinical Electrophysiology*, 2017.

[2] R. El Berbari, N. Kachenoura, F. Frouin, A. Herment, E. Mousseaux, and I. Bloch, "An automated quantification of the transmural myocardial infarct extent using cardiac de-mr images," in *Engineering in Medicine and Biology Society, 2009. EMBC 2009. Annual International Conference of the IEEE*. IEEE, 2009, pp. 4403–4406.

[3] J. D. Schuijf, T. A. Kaandorp, H. J. Lamb, R. J. van der Geest, E. P. Viergever, E. E. van der Wall, A. de Roos, and J. J. Bax, "Quantification of myocardial infarct size and transmurality by contrast-enhanced magnetic resonance imaging in men," *The American journal of cardiology*, vol. 94, no. 3, pp. 284–288, 2004.

[4] E. Heiberg, H. Engblom, M. Ugander, and H. Arheden, "Automated calculation of infarct transmurality," in *Computers in Cardiology, 2007*. IEEE, 2007, pp. 165–168.

[5] J. Alexandre, E. Saloux, A. E. Dugué, A. Lebon, A. Lemaitre, V. Roule, F. Labombarda, N. Provost, S. Gomes, P. Scanu, *et al.*, "Scar extent evaluated by late gadolinium enhancement cmr: a powerful predictor of long term appropriate icd therapy in patients with coronary artery disease," *Journal of Cardiovascular Magnetic Resonance*, vol. 15, no. 1, p. 12, 2013.

[6] P. Mountney, J. M. Behar, D. Toth, M. Panayiotou, S. Reiml, M. P. Jolly, R. Karim, L. Zhang, A. Brost, C. A. Rinaldi, and K. Rhode, "A planning and guidance platform for cardiac resynchronization therapy," *IEEE Transactions on Medical Imaging*, vol. 36, no. 11, pp. 2366–2375, Nov 2017.

[7] S. R. Stauffer and N. A. Peppast, "Poly (vinyl alcohol) hydrogels prepared by freezing-thawing cyclic processing," *Polymer*, vol. 33, no. 18, pp. 3932–3936, 1992.

[8] R. Karim, P. Bhagirath, P. Claus, R. J. Housden, Z. Chen, Z. Karimaghaloo, H.-M. Sohn, L. L. Rodríguez, S. Vera, X. Albà, *et al.*, "Evaluation of state-of-the-art segmentation algorithms for left ventricle infarct from late gadolinium enhancement mr images," *Medical image analysis*, vol. 30, pp. 95–107, 2016.